General Disclaimer

One or more of the Following Statements may affect this Document

- This document has been reproduced from the best copy furnished by the organizational source. It is being released in the interest of making available as much information as possible.

- This document may contain data, which exceeds the sheet parameters. It was furnished in this condition by the organizational source and is the best copy available.

- This document may contain tone-on-tone or color graphs, charts and/or pictures, which have been reproduced in black and white.

- This document is paginated as submitted by the original source.

- Portions of this document are not fully legible due to the historical nature of some of the material. However, it is the best reproduction available from the original submission.

X-613-69-494
PREPRINT

NASA TM X- **63781**

ROCKET SPECTROSCOPY
OF ZETA PUPPIS

ANDREW M. SMITH

NOVEMBER 1969

GSFC —— GODDARD SPACE FLIGHT CENTER ——
GREENBELT, MARYLAND,

ROCKET SPECTROSCOPY OF ZETA PUPPIS

Andrew M. Smith

Goddard Space Flight Center
National Aeronautics and Space Administration
Greenbelt, Maryland

ROCKET SPECTROSCOPY OF ZETA PUPPIS

ANDREW M. SMITH

Goddard Space Flight Center
National Aeronautics and Space Administration
Greenbelt, Maryland

Received:_____

ABSTRACT

A spectrum of ζ Pup extending from 920 to 1360$\overset{\circ}{A}$ with approximately 0.8$\overset{\circ}{A}$ resolution has been recorded at rocket altitudes. Tentative identification of 102 multiplets of both stellar and interstellar origin has been made, from which it is concluded that all lines included in existing model atmospheres have been detected with the exception of those masked by telluric N_2 or strong P Cygni type profiles. Additional weak absorption lines indicate a wide range of ionization and excitation entirely consistent with observations in the visible spectral region of similar type stars; they also appear to affect sensibly the energy distribution within the spectrum. Transitions in C III (λ1176$\overset{\circ}{A}$), N III (λ990, 92$\overset{\circ}{A}$), N IV (λ955$\overset{\circ}{A}$), N V (λ1239, 43$\overset{\circ}{A}$), O IV (λ1339, 43$\overset{\circ}{A}$), O VI (λ1032, 38$\overset{\circ}{A}$), and S VI (λ933, 44$\overset{\circ}{A}$) have been observed as P Cygni profiles. Excepting the S VI lines the mean radial velocities associated with ground state transitions and the transition from the lowest triplet state in

C III are close to an average velocity of 1770 km sec^{-1};
the mean radial velocities of the N IV and O IV ions
are 530 and 150 km sec^{-1} respectively. These results
suggest a positive velocity gradient in the observed
portion of the circumstellar envelope, and that the
escaping ions are loosely bound together with essentially
no difference in their average acceleration away from
the star. The interstellar columnar density of atomic
hydrogen was found to be (7.6 ± 2.5) 10^{19} cm^{-2}, the
quoted uncertainty being due only to the uncertainty
in establishing the continuum. The mean atom density
becomes (6.4 ± 2.1) 10^{-2}cm^{-3} if an interstellar distance
through atomic hydrogen of 390 pc is assumed.

I. INTRODUCTION

In March 1968 the ultraviolet spectrum of ζ Pup (O5f) was recorded at rocket altitudes with wavelength coverage extending from 921 to 1360Å at about 0.8Å resolution. Presented in this paper are the results which have been discussed with the following objectives in mind:

1. It is desirable to establish the degree of consistency between the observed weak lines and those appearing in the visual spectra of similar type stars.

2. A comparison between the observed strong ultraviolet lines and those included in existing model atmospheres for O5 stars may be made, particularly with a view to estimating the sufficiency of the model lines to account adequately for line blanketing.

3. P Cygni type profiles may be examined with the hope of extracting more information about the circumstellar envelope.

4. Interstellar lines can be identified, but with the exception of the Lyman-α line, cannot be reliably analyzed. A determination of the columnar density of atomic hydrogen can be made, and the result, contingent upon the value of the interstellar distance through atomic hydrogen, can be compared with a model of the interstellar medium.

- 4 -

II. THE EXPERIMENT

The instrumental payload was nearly identical to
that described previously (Smith, 1969) with substantial
improvements being made in the pointing control system
only. Briefly, the spectrograph itself consisted of a
single, concave objective grating used in the so-called
Wadsworth mount configuration with the characteristics
listed in Table 1.

Table 1
Rocket Spectrograph Characteristics

Focal length	24.9 cm
Grating size (aperture)	2 cm x 7 cm
Grating line density	1200 mm^{-1}
Grating coating	Pt
Field of view normal to dispersion plane	$\pm$ 1/2°
Field of view in dispersion plane	$\pm$ 1.0°
Laboratory resolution at λ1134$\overset{\circ}{A}$	1/4$\overset{\circ}{A}$
Plate factor ($\sim$ linear)	33.4$\overset{\circ}{A}$ mm^{-1}

Kodak Pathe SC5 film was used, and the development
procedure included slight agitation of the exposed film
for 2 minutes in D19B at 68°F. A calibration curve is
presented in Figure 1 in which the log of the exposure
is plotted along the abscissa, and the film density
averaged over the densitometer slit height is plotted on
the ordinate. In deriving the calibration curve the

assumption was made that there was no reciprocity failure
at the short wavelengths of this experiment (Fowler, Rense,
and Simmons, 1965). This assumption permitted holding
the source intensity constant while varying the exposure
time thus greatly simplifying the calibration procedure.
It should be noted that though the slope of the calibration
curve seemed to be relatively constant for different film
samples and throughout the recorded wavelength range the
location of the curve along the exposure axis varied
by as much as a factor of 2. The spread of data points
about the solid curve gives an indication of the uncertainty
involved in the instrument calibration. If it is assumed,
however, that the calibration is sufficiently accurate
to find the Lyman-α line profile, then for this purpose
the dynamic range of the instrument is about a factor of
5.

The payload was launched by an Aerobee 150 rocket
from White Sands, N. Mex. on March 21, 1968 at 2024 (MST).
Two exposures were secured, one at a mean altitude of
190 km for 214 sec, and another at 123 km for 68 sec.
The fluctuation of the pointing direction about the earth-
star line was within ± 11 seconds of arc both in the
plane and normal to the plane of dispersion. This was
achieved by the "STRAP III" attitude control system
provided by the Goddard Space Flight Center.

Upon development of the flight film it was found that

the second and short exposure possessed a background fog,
most certainly arising from a light leak, which became
progressively more dense with decreasing wavelength.
For this spectrogram the signal is still discernible at
$\lambda > 990$Å, but is only used at $\lambda > 1200$Å principally to verify
strong features identified on the long exposure spectrogram
for which background fog, if any, is indistinguishable
from clear plate noise. The wavelength scale for the long
exposure was determined by fitting the identified features
produced by telluric $N_2 (\sim \lambda 960$Å$)$, interstellar N I$(\lambda 1134.6$Å$)$
and interstellar Si II$(\lambda 1304.4$Å$)$ to a quadratic function
of the distance measured on the film along the spectrum
from an arbitrary starting point. The resulting scale
is thought to be accurate within 0.3Å. The resolution
of the spectrograms is 0.8Å or perhaps slightly better
(0.7Å), and limited by the pointing fluctuations.

III. THE RESULTS

An enlarged reproduction of both spectrograms appears
in Figure 2 with the strongest features identified.
Figure 3 contains in three sections the microdensitometer
traces of both spectrograms which have been smoothed in
a computer using a triangular weighting function 0.62$\overset{o}{\text{A}}$
full width at half maximum. In Figure 2 and in Figure 3
at $\lambda > 1224\overset{o}{\text{A}}$ data from the short exposure appear above the
data of the long exposure, and the effect of the background
fog in the former can easily be seen. The multiplets
shown in Figure 3 include at least one transition which
correlates with an observed spectral feature. Generally,
all transitions of a given multiplet are indicated, but
in a few cases some members have been excluded for
purposes of clarity. The top spectrum appearing in
Figure 3 corresponds to the model calculations of Hickok
and Morton (1968) with $T_e = 37450^{o}K$ and log g = 4.00.
In this case the ordinate is in flux units.

There are some features in the observed spectra which
can be attributed to constituents of the earth's atmosphere
or, as in the case of water vapor, of the residual gas
in the vicinity of the rocket during flight. As reported
in an earlier observation of α Vir (Smith, 1969) the
absorption bands of N_2 are very strong at wavelengths
less than $\lambda 1000\overset{o}{\text{A}}$ those near 960, 966, and 972$\overset{o}{\text{A}}$ being
particularly obvious. In fact, it seemed in the present
case that these bands were chiefly responsible for the

- 8 -

shape of the spectrum in this region, and were therefore used in the determination of the wavelength scale. The molecule O_2 also possesses absorption bands at these short wavelengths, specifically at 939, 948, 956, 966, 972 and 983Å, but those of N_2 are expected to be stronger. An O_2 band at $\lambda 1244$Å should, however, be seen in the short exposure at relatively low altitudes. Unfortunately, the data quality is poor, but a N V emission feature appearing in the long exposure at 1243Å is missing in the short exposure, and the absence may be due to absorption from O_2 at this wavelength. The resonant line of OI at $\lambda 1302.2$Å is present in the spectrum and many originate in the earth's atmosphere. However, the two other lines of this triplet ($\lambda\lambda 1304.9$, 1306.0Å) which should be observable if indeed the absorption is telluric cannot be plausibly correlated with any observed feature. Thus, at least most of the observed 1302.2Å absorption is thought to have an interstellar origin.

The features at 1018, 1056, 1113 and 1220Å are attributed to absorption bands of H_2O adsorbed by the rocket and payload surfaces while on the ground and at low altitudes, and evaporated into the optical environment at the exposure altitudes.

It should be remarked that the emission-like feature in the center of the Lyman-α line of the long exposure is a film blemish, and can be seen as such in the spectrogram reproduction of Figure 2. Finally, in the long exposure

the increase in intensity culminating in a sharp peak near $\lambda 1327\mathring{A}$ is thought to be spurious particularly in view of the fact that such behavior does not occur in the short exposure. There is also a film blemish in the neighborhood of this feature in the long exposure which might have extended into the spectrum thereby influencing the densitometer reading.

The identified spectral lines are listed in Table 2. Column 1 contains the ion identification together with a multiplet or line reference. Regarding the latter a number refers to the compilations of Moore (1950, 1965), a K refers to the emission line tables of Kelly (n.d., 1968), an H indicates that the paper of Hickok and Morton (1968) was used, P refers to an article of Palenius (1967), and HA to the work of Hallin (1966). Laboratory measured wavelengths of the identified transitions and the observed wavelengths of the corresponding spectral features are listed in columns 2 and 3 respectively, and the excitation potentials in column 4. For those transitions exhibiting P Cygni type profiles the wavelength at the center of the absorption component   followed by the wavelength corresponding to the blue emission edge are noted in column 3. Listed in column 5 are gf values taken from Varsovsky (1961), Allen (1963), Wiese, Smith, and Glennon (1966), and Garstang and Shamey (1967). No blends have been indicated simply because most lines are observed to be blends of two or more plausible transitions, and

- 10 -

in those cases where only one transition correlates with
an observed feature it is likely that other as yet
unrecognized transitions do as well.

IV. DISCUSSION

The following paragraphs contain remarks on the lines of the various ions identified in the recorded spectra.

HI - Most of the absorption in the Lyman lines must be due to interstellar hydrogen. All the Lyman lines through Ly-θ except Ly-α and Ly-δ are masked by much stronger lines in the spectrum.

He II - The transition at λ949.3Å may contribute to the feature near λ949.9Å. All other transitions throughout the measured spectrum are masked to some extent by stronger absorption and emission features. No emission in He II can be identified.

C I, II, III, IV - Of the six resonance lines in C I listed in Table 2 for which some evidence is found the identification of only two at 1277.2 and 1280.2Å can be considered probable.

There is mediocre evidence for two resonance lines in C II at 1036.3Å and 1334.5Å which are presumably interstellar in origin. The well observed C III (λ1175.7Å) line is seen as a P Cygni profile with weak emission, and modified by the unshifted absorption line. The same kind of profile might be expected at 977.0Å where a resonant transition in C III exists. Evidence for an unshifted absorption line at this wavelength is good, but the expected P Cygni profile will be masked by other absorption lines and bands. The unshifted, subordinate lines of C III at 1175.7Å, 1247.4Å, and 1296.3Å originate

- 12 -

in the stellar atmosphere, and in the case of the 1175.7Å
line the optical depth at this wavelength in the circumstellar
envelope is not sufficiently large to prevent seeing to
the "surface" of the star.

There is weak evidence for C IV near λ1108.0Å. Weak
lines near λ1169.0 and 1198.6Å might be expected; however,
in both cases strong absorption from C III (λ1168.8Å)
and N I (λ1199.9Å) predominate in the respective wavelength
regions. The lines of C IV at 948.1 and 948.2Å are also
not observed. The highest excitation observed in any
of the carbon ions is 39.5 eV in C IV.

N I, II, III, IV, V - Preliminary calculations show that
the N I lines at 1134.6Å and 1199.9Å must be telluric
as well as interstellar in origin.

The absorption feature at 1084.3Å is probably due
to the combined effect of N II (λ1084.0Å), a resonance
transition, and He II (λ1085.0Å). It is improbable that
N II is abundant in the stellar atmosphere, and since
the ionization potential of N I is 14.5 eV it is also
improbable that N II will occur in the H I regions of
interstellar space. Thus, almost all of the N II producing
the feature at 1084.3Å must be located in the H II
region surrounding ζ Pup.

The N III doublet .t 991.0Å originates in the ground
state configuration, and exhibits a P Cygni profile with
the emission and absorption features probably influenced
by telluric N_2 and Cl III absorption respectively. The

- 13 -

weak unshifted absorption features identified in Table 1
with subordinate lines in this ion must arise within the
stellar atmosphere.

There is considerable evidence in the spectrum for
the existence of subordinate lines of N IV, and these
are listed in Table 1. Such lines at 1168.6, 1169.1,
and 1169.5Å for which poor evidence exists are masked
by   shifted C III (λ1175.7Å) absorption at 1168.8Å.
The transition at 955.3Å exhibits a relatively weak P Cygni
profile. The lower level is at 16.1 eV, and may decay
radiatively to the ground state ($2p\ ^1P^o \rightarrow 2s^2\ ^1S$) with
gf = 0.64. The most likely way that the $^1P^o$ level may
be populated is by ordinary thermal processes. This
implies that the radiation field cannot be significantly
diluted, and that the excited N IV ions must therefore
be close to the "surface" of the star. Morton (1969)
has also reached this conclusion. A multiplet of N IV
at 923.2Å is mainly responsible for terminating the
observed spectrum near 921Å; it should also exhibit a
P Cygni profile. The range in observed excitation of
atmospheric N IV is large extending from 23.3 eV to 61.7 eV.

Perhaps the strongest feature of the recorded
spectrum is the circumstellar P Cygni type profile of
N V (λ1238.8, 42.8Å). On the other hand, the evidence
for the subordinate lines of N V at 1049.6 and 1048.2Å is
weak, but if accepted indicates the highest observed
state of excitation, namely 76.3 eV.

O III, IV, VI - Evidence for only four subordinate lines
of O III as listed in Table 2 has been found, the maximum
observed excitation in this ion being 26.1 eV.

The O IV lines at 1338.6, 1343.0 and 1343.5Å are
strong and show a displacement to shorter wavelengths;
apparently there is a small red shifted emission feature
associated with the 1343.0-3.5Å transition. As in the
case of the N IV (λ955.3Å) P Cygni profile this transition
originates in an excited level of 22.3 eV which can decay
radiatively to the ground state ($2p^2$ $^2P \rightarrow 2p$ $^2P^o$) with
gf = 2.28. If the population of the 22.3 eV level is by
thermal processes then the excited O IV ions must be
close to the "surface" of the star.

The P Cygni type profile near 1030Å associated
with the resonance lines of 1031.9 and 1037.6Å in O VI
is nearly as strong as the P Cygni profile associated
with the 1238.8 and 1242.8Å lines in N V. The profile
is modified by absorption of interstellar C II at 1036.3Å,
and possibly by a P IV line at 1031Å. If the influence
of the latter is small it is likely that the absorption
components of the doublet are partially resolved, and the
profile may prove useful for a mass loss estimate.
Si II, III, IV - Lines in Si II at 1260.4 and 1304.4Å are
definitely observed, and are likely to be interstellar
in origin. Their profiles, however, are modified by line
absorption at nearby wavelengths, and estimates of the
interstellar abundance of Si II are unreliable. Other

resonance lines in this ion appear at 1190.4 and 1193.3Å but their identification is uncertain.

The resonant Si III line at 1206.5Å appears as a weak but definite absorption line in this data, but cannot plausibly be associated with a shortward-shifted feature at 1200Å as suggested by Morton, Jenkins and Brooks (1969). The latter feature certainly exists, but can be attributed exclusively to the combined effect of interstellar and telluric absorption in N I and absorption in three lines near 1201Å originating in the ground state configuration of S III. The plentiful, weak subordinate lines in Si III are listed in Table 2, and exhibit a range in excitation extending from 6.5 eV to 32.1 eV.

Relatively strong subordinate lines in Si IV are found in one multiplet at 1128.3 and 1122.5Å, and in another at 1066.6Å. The four other tentatively identified multiplets of this ion contain weak lines with excitation extending to 27.1 eV. . No resonance lines of Si IV are found in the recorded wavelength region.

P III, IV, V   There is some evidence for ground state transitions in P III at 998.0 and 1003.6Å, however, the doublet in this ion at 1334.8-44.9Å is probably masked by the effects of interstellar C II and circumstellar O IV absorption. There is only one other tentatively identified multiplet of P III near 1051Å, the excitation being 9.3 eV.

The resonance line in P IV at 950.7Å very likely contributes to the feature at 949.9Å together with transitions in H I (Lyman-δ) and He II (λ949.3A). The P IV lines at 1030.5 and 1035.5Å may contribute to the features near these wavelengths, but it is thought that these features are predominately due to shortward-shifted O VI absorption at 1037.6Å and interstellar absorption in C II at 1036.3Å respectively. The remaining weak lines in P IV indicate a maximum observed excitation of 31.9 eV.

Resonance transitions in P V have reliably been identified at 1118.0 and 1128.0Å, and subordinate lines indicating 25.3 eV of excitation in P V have tentatively been identified at 997.6 and 1000.4Å.

S II, III, IV, VI - There is weak evidence for interstellar S II where resonance transitions occur near 1255Å.

Good evidence exists for the presence of the resonance transitions in S III near 1020 and 1200Å. Generally, mediocre evidence for subordinate lines in S III exists indicating a maximum observed excitation of 12.2 eV.

Ground state transitions in S IV at 1063 and 1074Å are clearly seen, but appear to be considerably weaker than the corresponding lines in the model spectrum. The discrepancy most likely illustrates the difficulty in determining the proper damping constants to use in model calculations. Subordinate lines in S IV reveal a maximum observed excitation of 16.6 eV. The strongest features due to sulphur, however, arise in the circumstellar envelope, and are the P Cygni type profiles associated with the

transitions in S VI at 933.4 and 944.5Å.

C1 III, C1 IV - The resonance lines in Cl III near λ1010Å
are weak if indeed detectable. Three lines at 985.8,
985.0 and 973.2Å in Cl IV which should be observable
are likely to be masked by the N III (λλ989.8, 91.6Å) P Cygni
profile and a strong telluric N_2 (λ972.1Å) band. It is
also likely that the shape of the spectrum near 977.0Å
where ground state transitions in Cl IV (λλ977.6, 7.9Å)
may produce some observable effect is determined chiefly
by the strong resonance transition in C III at 977.03Å.

Ar IV - Mediocre evidence for transitions in Ar IV
ions with an excitation of 4.3 eV is noted near 1187.8,
1190.4 and 1197.8Å.

Fe II, III, IV - the only plausible evidence for Fe II,
presumably of interstellar origin, is near 1142Å and
possibly 1096Å. Other possible resonance lines either
do not correspond to features in the spectrum or correspond
to features primarily due to other ions.

There is good evidence in the spectrum for transitions
from the ground state configuration in Fe III at 1124.9Å.
The gf-value of the resonance transition at 1122.5Å is
about twice that for the 1124.9Å transition; consequently,
the resonance transition probably contributes to the
moderate absorption feature at 1122.5Å.

A multiplet of Fe IV near 1270Å is the only apparent
evidence for this ion throughout the observed spectral

- 18 -

range which includes no resonance lines. The excitation
of the ion for the observed multiplet is close to 21 eV.

Some features which are likely to be caused by some
absorption agent, but for which none at all could be found
are listed in Table 3. Notable are two weak emission-
like features at $\lambda\lambda 1226.5$ and $1094.2\mathring{A}$ which seem to
have some correlation with similar features on the short
exposure. If these are not spurious effects no plausible
explanations can be made at the present time.

Table 3

Unidentified Lines in the UV Spectrum of ζ Pup

$\lambda(\mathring{A})$ Measured	$\lambda(\mathring{A})$ Measured	$\lambda(\mathring{A})$ Measured	$\lambda(\mathring{A})$ Measured
1357.7 * m	1306.5 w	1221.5 v	1091.0 v
1352.8 w	1266.0 w	1104.7 v	1080.0 v
1350.0 w	1257.7 w	1102.6 v	1075.7 v
1346.1 w	1226.5 e	~1100 +v	1017.7‡v
1320.8 w	~1225 v	1094.7 v	1000.6 v
1311.7 w	1222.9 v	1094.2 e	

* The strength of the feature is moderate, m; weak, w;
  very weak, v; the feature appears in emission, e.

+ The feature is a blend of weak lines.

‡ This line may be due to H_2O.

Summarized in Table 4 are the data concerning the
P Cygni type profiles measured in the present experiment.

Table 4

Characteristic Radial Velocities of Ions in the
Circumstellar Envelope of Zeta Puppis

Ion	C III	N III	N IV	N V	O IV	O VI	S VI
Laboratory Wavelength($\overset{\circ}{A}$)	1175.7	989.8 991.5 991.6	955.3	1236.8 1242.8	1338.6 1343.0 1343.5	1031.9 1037.6	933.4 944.5
Central Velocity (km sec^{-1})	1760 (1860)	1820	530 (780)	1670 (1550)	150	1830	1380
Extrapolated Maximum Velocity (km sec^{-1})	3200	3300	1500	3300	1300	3500	2500

For the purposes of this table only the velocities
derived from the profile corresponding to the 933.4$\overset{\circ}{A}$
transition in S VI are listed. The emission associated
with this transition would cause an underestimation of
the mean radial velocity of S VI ions as determined from
the shortward-shifted 944.5$\overset{\circ}{A}$ absorption line. The contributions
of the Cl IV (λ985$\overset{\circ}{A}$) line to the N III (λ991$\overset{\circ}{A}$) profile
and a P IV multiplet near 1031$\overset{\circ}{A}$ to the O VI (λ1032, 38$\overset{\circ}{A}$)
profile have been assumed negligible. The extrapolated
maximum velocities are of course quite uncertain.

Morton, Jenkins and Brooks have determined radial

velocities for three of the ions contained in Table 4; their results appear in parenthesis, and indicate substantial agreement with the present results. In the case of N IV it is noteworthy that these authors observed a transition at 1719Å which originates at the same excited level (2p $^1P^o$, 16.13 eV) as does the 955Å transition reported here.

For the purpose of calculating the columnar density of atomic hydrogen the calibration curve of Figure 1 was used to obtain the relative flux distribution in the wavelength interval between 1194 and 1236Å. The results are given by the solid line in Figure 3. Other sources of line absorption including the shifted absorption component of the circumstellar N V (λ1239, 43Å) doublet have been identified in the figure, and quite obviously pose a difficult problem in the determination of that part of the profile due exclusively to Lyamn-α absorption. In order to make this distinction the shape of the inter-stellar line was assumed to be of the form

$$I(\lambda)/I_o = \exp[-C\ H(a,u)] \qquad (1)$$

where I_o is the flux in the stellar continuum, $H(a, u)$ is the Harris function and C is defined by the relation

$$N\ell = \frac{C}{\pi} \cdot \frac{mc}{e^2} \cdot \frac{\Delta\nu_o}{f} . \qquad (2)$$

Here, N is the mean number density of hydrogen atoms, and ℓ is the interstellar distance through atomic hydrogen. The other symbols in equations (1) and (2) have their usual meanings (Aller, 1963). In the case of the heavily saturated Lyman-α line the observed profile is

determined essentially by radiation damping, the doppler
width $\Delta\lambda_o$ being very small, i.e. about 0.05Å for a temperature
of $10,000^oK$. Thus, the exponent in equation (1) reduces
to (-)$Ca/\pi u^2$ which is independent of temperature. On
the assumption of a value for I_o profiles for various
values of C were computed, and the best value of C was
selected on the basis of the best fit between the computed
and measured profiles in the core of the Lyman-α line.
The dashed lines in Figure 4 illustrate the procedure
showing both the assumed continuum and the best-fit
computed profile. It was hoped that in this way the
effects of line absorption in the vicinity of the inter-
stellar Lyman-α line could be significantly reduced.

Application of equation (2) gives the final result
of N = $(7.6 \pm 2.5)10^{19}$ cm^{-2}, the quoted error being due
exclusively to the estimated uncertainty in establishing
the continuum level. Adopting the value for ℓ of 390 pc
suggested by Morton, Jenkins and Brooks N becomes
(0.064 ± 0.021) cm^{-3}. The equivalent width is of interest
when a comparison with other results is to be made. It
can be easily deduced from the value of $N\ell$, and is 6.4Å.

V. SUMMARY AND CONCLUSIONS

Evidence for all the lines used in the Hickok and Morton model has been found except for those either masked by N_2 absorption bands or by strong P Cygni type profiles. Some observed lines, however, appear to be considerably weaker than the corresponding model lines - the S IV doublet near 1070Å is an example - and this circumstance most likely reflects an uncertainty in the damping constants to be used in the model calculations. All of these lines originate at ground or low lying levels. Most of the identified features, however, correspond to subordinate lines which exhibit both a wide range in ionization and excitation. As an example, Table 2 shows that lines of N III (λ980Å), N IV (λ1079Å), and N V (λ1048, 50Å) originate at levels of 12.5, 53.0, and 76.3 eV respectively. Further, it may be stated qualitatively that line blanketing from the weak lines in the observed spectral region is sufficient to affect the energy distribution in the spectrum. This is particularly noticeable in the wavelength intervals extending from 998 to 1015Å and from 1190 to 1210Å.

These results are in essential agreement with spectral observations carried out in the visible on similar type stars. For example, N V has been identified in the spectrum of HD 190429 (O5f) by Swings and Struve (1940, again in the same star by Oke (1954), and in 9 Sge (O7)

by Underhill (1958). In addition, Miss Underhill has
tentatively identified the presence of O VI in 9 Sge.
Both of these stars exhibit lines of N III and N IV, and
in 9 Sge O III and O IV are definitely present while
O V is probably present. Likewise, the range of excitation
in the atmospheres of these stars is similar to that
revealed in the ultraviolet spectrum of ζ Pup. Thus,
the observed excitation of the N V ions in the atmosphere
of HD 190429 extends from 56.3 to 59.0 eV, and the
excitation of the O VI ions tentatively identified in
9 Sge is over 100 eV.

The similarity between the ultraviolet and visible
observations may be carried further by noting that the
excitation of N IV and Si IV ions revealed by the many
ultraviolet lines is close to, or equal to the
excitation revealed in these ions by visible spectra.
For example, the ultraviolet Si IV lines in the ζ Pup
spectrum at 1211 and 1212Å originate in the same lower
level as the visible lines in the spectrum of 9 Sge (O7)
at 4089 and 4116Å; the excitation is 24.0 eV. Swings
and Struve observed these last two lines as P Cygni type
profiles in HD 190429 (O5). Similarly, the N IV lines
of ζ Pup at 1133 and 1136Å originate in the same level
as the visible lines at 3479-85Å in the spectra of both
9 Sge and HD 190429; the excitation in this case is 46.6 eV.
Neglecting the possibility of a time variation in spectral
characteristics and avoiding wavelengths where strong

absorption occurs we can plausibly conclude that in both the ultraviolet (921-1360Å) and the visible we see to atmospheric levels with physical parameters sufficiently the same to produce identical ions. The geometrical extent of the atmosphere over which the appropriate physical parameters exist is probably large; nevertheless, these results are consistent with the fact that the principal source of continuous opacity in the early O stars is free electron scattering, and thus varies only slowly with wavelength.

No evidence has been found for narrow unshifted emission lines similar to those of He II (λ4686Å), N III (λ4634, 42Å) and C III (λ5696Å) characteristic of Of stars in this or any other ultraviolet spectrum of ζ Pup. A probable explanation is that no selective excitation processes such as the familiar fluorescence mechanisms which require large fluxes of HeII and HI Lyman-α quanta are operating at wavelengths less than 1965Å. As one might expect, however, it is very difficult to establish a suitable continuum flux level, and consequently it is impossible to detect weak emission in the present data with reasonable certainty.

It was pointed out in § IV that the P Cygni profiles produced in N IV ions near 955Å and in O IV ions near 1340Å very likely arise close to the stellar atmosphere where dilution effects are still weak. The mean radial velocities of these ions are relatively small being 530

and 150 km sec^{-1} respectively. On the other hand, the
lower level of the transition associated with the P Cygni
profile in C III near 1176Å is metastable. It can be
populated only under conditions where the radiation field
is dilute, that is, when the C III ions are at distances
on the order of several stellar radii from the center of
the star. In distinction with the excited N IV and O IV
ions the C III ions possess a relatively large mean
radial velocity of 1760 km sec^{-1}. It may also be noted
that for any plausible atmospheric temperatures and
pressures there should be no appreciable atmospheric
abundances of N V or O VI, and yet the data indicate
a large abundance of these ions in the circumstellar
envelope. It is reasonable to assume that N V and O VI
with mean radial velocities close to 1800 km sec^{-1} occur
with maximum probability well beyond the unaccelerated
atmosphere where suitable conditions exist, that is,
high electron temperatures and low electron densities
when compared to photospheric values. These data are
usually   interpreted as evidence for a positive velocity
gradient in the detectable part of the circumstellar
envelope.

Table 4 shows that not only do ground state ions
observed in the circumstellar envelope possess escape
velocities, but that their mean radial velocities with
the exception of S VI are comparable; the average is 1770

km sec^{-1}. Ions of C III in the metastable state at 6.5
eV have a mean radial velocity of 1760 km sec^{-1}, nearly
identical with the average of the ground state ions. In
addition to the values quoted in Table 4, Morton, Jenkins,
and Brooks have measured mean radial velocities of 1840
and 1810 km sec^{-1} for the ions of C IV and Si IV respectively.
Their average mean radial velocity for ground state ions
is 1730 km sec^{-1}. The similarity of these results
including both the ground state ions of C IV, N III,
N V, O VI, and Si IV and the excited C III ions is
noteworthy, particularly when it is realized that the
density distribution with distance from the star of each
ion can well account for the velocity differences between
ions. It should also be noted that the difficulty in
establishing the position of the minimum residual intensity
in the   shifted absorption feature will produce at
best an uncertainty in the corresponding velocity estimate
of $\pm$100 km sec^{-1}. For the highly saturated lines this
uncertainty is larger. The deficit in the mean radial
velocity of S VI ions when compared to the average value
is 390 km sec^{-1}. It may be due to the influence of some
unrecognized source of absorption or emission near the
S VI (λ933, 45Å) lines, the density distribution of these
ions in the circumstellar envelope, or a combination of
both effects. The deficit, however, may occur for some
entirely different reason, and this uncertainty reflects
a rather unsatisfactory understanding of the circumstellar

envelope. In spite of the anomolous characteristic of the S VI lines, the data suggest that the escaping ions are at least loosely bound together in a circumstellar plasma with essentially no difference in the average acceleration of the various individual particles.

It is probable that the degree of ionization increases with increasing distance from the stellar surface but the lower levels of ionization as evidenced by the strong N III P Cygni profile at 991Å are not completely depleted. The C III (λ977Å) transition should also be seen as a P Cygni profile since the ionization potentials of N III and C III are about the same, that is 47.2 and 47.7 eV respectively. The data are indeed consistent with this prediction, but are as noted in §III confused by the presence of a telluric N_2 absorption band. On the other hand, the Si III (λ1207Å) resonance line is not seen in the present observation as a P Cygni profile. The ionization potential for this ion is 33.3 eV, and on the basis of these facts one would not expect to find S III (I. P. = 34.9 eV) ions in the interstellar envelope, but would find O III (I. P. 54.7 eV) ions there. It is reasonable to expect that N IV exists in the ground state at roughly the same distances and velocities as N III and N V. We do not detect it because the resonance transitions lie at wavelengths less than 912Å which are hidden from view by interstellar atomic hydrogen. For the same reason the ions of C V, O III, O IV, and O V, which can be

expected in the circumstellar envelope cannot be observed.

Again, the visual data and the ultraviolet data can
be considered self-consistent with respect to emission
lines and P Cygni profiles. The visible emission lines
characteristic of Of stars very likely originate high in
a hot rarified atmosphere (Oke, 1954), yet with a geometrical
dilution factor still close to unity. These same lines
may possess a broad, weak emission component with a
maximum extent corresponding to radial velocity values
in excess of 1000 km sec^{-1} in λ Cep (06f) (Wilson,
1958), and from 500 to 1000 km sec^{-1} in 9 Sge (07)
(Underhill, 1958). In the latter case the N III (λ4634-40Å)
line seems to appear as a P Cygni type profile, and in
the case of HD190429 (05f) Swings and Struve have noted
P Cygni type profiles of high excitation lines in N IV (λ4057Å),
N V (λ4603, 19Å) and Si IV (λ4098, 116Å) with radial
velocity values of 182, 169, and 161 km sec^{-1} respectively.
These features arise presumably beyond the levels wherein
the sharp characteristic lines are formed in a region
where radial acceleration of the atmosphere has already
begun. Here the N IV lines at 955 and 1719Å and the O IV
lines at 1339 and 1344 are also formed. Further out where
the dilution factor has decreased significantly, population
of the ionic ground states is preferred. However, even
at these distances, perhaps 2 or 3 stellar radii from the
center of the star, there is some excitation as evidenced
by the spectrum of λ Cep.

The mean hydrogen atom density in the H I region between the sun and ζ Pup was determined to be (0.064 ± 0.021) cm^{-3} which is a factor of 3.1 smaller than the value of 0.2 cm^{-3} proposed by Field, Goldsmith, and Habing (1969) for the intercloud nuclei density. The observed value might reasonably be raised to 0.106 cm^{-3} by taking into account both the uncertainty in locating the continuum and the uncertainty in the contour fitting method described in $\S$ IV. On the other hand, the interstellar distance through atomic hydrogen (390 pc) may be too large. In view of these uncertainties it is concluded that the observed and model densities are at least consistent with each other, neither being implausible.

Fig. 1 - Calibration function of the rocket spectrograph.
The log of the exposure to Lyman-α light is plotted
in relative units along the abscissa, and the film
density averaged over the densitometer slit height
is plotted on the ordinate.

Fig. 2 - Two ultraviolet spectrograms of ζ Pup. The
exposure times of the top and bottom spectrograms
were 68 and 214 sec respectively. Some identifications
of the stronger features are shown, the numbers
indicating the approximate wavelengths in Angstrom
units.

Fig. 3 - Microdensitometer traces in three sections of the
ζ Pup spectrograms. The abscissae are in Angstrom
units, and the ordinates represent densities of the
214 sec exposure which appears at the bottom of
each section. A density of 0.24 corresponding to
the background value is indicated. The top spectrum
in each section corresponds to the model calculations
of Hickok and Morton (1968), and the ordinates (not
shown) are in relative flux units. At $\lambda > 1224\overset{o}{A}$ a
trace of the 68 sec exposure spectrogram is shown
between that of the 214 sec exposure and the model
spectrum.

Fig. 4 - Lyman-α line in the spectrum of ζ Pup. Wavelength
is plotted on the abscissa, relative flux values
on the ordinate. The solid line indicates the

measured relative flux distribution, and the dashed

contour is a computed profile fitted to the

observations in the core of the line. The dashed

horizontal line indicates the assumed position

of the continuum.

REFERENCES

Allen, C. W. 1963, *Astrophysical Quantities* (2nd ed., London: Athlone Press).

Aller, L. H. 1963, *The Atmospheres of the Sun and Stars* (2nd ed.; New York: The Ronald Press Co.), p 323.

Field, G. B., Goldsmith, D. W., and Habing, H. J. 1969, *Ap. J. (Letters)*, 155, L149

Fowler, W. K., Rense, W. A., and Simmons, W. R. 1965, *Appl. Opt.*, 4, 1596.

Garstang, R. H., and Shamey, L. J. 1967, in the *Magnetic and Related Stars*, ed. R. C. Cameron (Baltimore: Mono Book Corp.)

Hallin, R. 1966, *Arkiv Fysik*, 31, 511.

Hickok, F. R., and Morton, D. C. 1968, *Ap. J.* 152, 203.

Kelly, R. L. n.d., *Table of Emission Lines in the Vacuum Ultraviolet for all Elements*, University of California Radiation Laboratory 5612.

_____. 1968 *Atomic Emission Lines Below 2000 Angstroms*, U. S. Naval Research Laboratory Report 6648.

Moore, C. E. 1950, *N.B.S. Circ. No. 488*, Sec. 1.

_____. 1965, *N.S.R.D.S.-N.B.S. 3*, Sec. 1.

Morton, D. C. 1969, *Astrophysics and Space Science*, 3, 117.

Morton, D. C., Jenkins, E. B., and Brooks, N. H. 1969, *Ap. J.*, 155, 875.

Oke, J. B. 1954, *Ap. J.*, 120, 22.

Palenius, H. P. 1967, *Arkiv Fysik*, 34, 571.

Smith, A. M. 1969, *Ap. J.*, 156, 93.

Swings, P., and Struve, O. 1940, _Ap. J._, 91, 546.

Underhill, A. B. 1958, _Publ. Dominion Astrophys. Obs._, 11, 143.

Varsovsky, C. M. 1961, _Ap. J. Suppl._, 6, 75.

Wiese, W. L., Smith, M. W., and Glennon, B. M. 1966, _N.S.R.D.S.-N.B.S. 4_.

Wilson, R. 1958, _Publ. Roy. Obs. Edinburgh_, 2, No. 3.

Table 2
Identifications of Lines in the UV Spectrum of Zeta Puppis

Ion Multiplet	Laboratory	Measured	χ(ev)	gf
H I (4) *m	949.74	949.9	0.00	0.02788
H I (1) s	1215.67	1215.9	0.00	0.8324
He II (19) ≠,w,l	949.30 949.35	949.9	40.64	0.030808
He II (14) m	1084.91 1084.98	1084.3	40.64	0.35736
C I (19) ≠,i,v,p	1155.84 1156.06	1155.8	0.00	---
C I (12) i,v,p	1192.48	1192.9	0.00	---
C I (11) i,v,p	1192.92 1193.00	1192.9	0.00	---
C I (9) i,m,p	1260.75	1260.6	0.00	0.029
C I (7) i,w,l	1277.15	~1277	0.00	0.064
C I (5) i,w,l	1280.15	1280.1	0.00	0.020
C I (4) i,w,p	1328.82	1328.8	0.00	0.039
C II (2) i,w,l	1036.33	1036.3	0.00	0.12
C II (1) i,w,l	1334.52	1334.4	0.00	0.52
C III (1) w,l	977.03	~ 977	0.00	0.81

Multiplet	Laboratory	Measured	χ(ev)	gf
C III (K) v,p	1165.70 1165.87	1165.7	22.62	---
C III (4) c	1174.92		6.46	0.33
	1175.25		6.46	0.26
	1175.57	1168.8	6.46	0.20
	1175.70	1176.7	6.47	1.00
	1175.97		6.46	0.26
	1176.35		6.47	0.32
C III (9) w,l	1247.37	1247.2	12.64	0.27
C III (K) w,p	1296.30	1296.0	33.33	---
C III (K) v,p	1308.73	1309.0	22.62	---
C IV (K) w,p	1107.60 1107.93	1108.0	39.51	---
N I (2) i,m	1134.17		0.00	0.096
	1134.42	1134.6	0.00	0.19
	1134.98		0.00	0.26
N I	1199.55		0.00	0.72
	1200.22	1200.3	0.00	0.44
	1200.71		0.00	0.24
N II (1) i,m	1083.98	1084.3	0.00	0.17
	1084.57		0.01	0.13
	1084.57		0.01	0.39
	1085.54		0.02	0.12
	1085.70		0.02	0.70
N III (12) w,l	979.77		12.47	0.08
	979.84	979.7	12.47	0.72
	979.92		12.47	1.12
	980.01		12.47	0.08

Table 2 (cont'd.)

Ion Multiplet	λ(Å) Laboratory	λ(Å) Measured	χ(ev)	gf	Ion Multiplet	λ(Å) Laboratory	λ(Å) Measured	χ(ev)	gf
N III	989.79	985.0	0.00	0.36	N IV	1270.28	1270.0	50.11	---
(1) c	991.51	990.3	0.02	0.07	(K) w,p	1272.16		50.11	---
	991.58		0.02	0.65		1272.74	1273.0	50.11	---
						1273.47		50.11	---
N III	1005.98	1005.9	16.17	0.36		1273.72		50.11	---
(17) w,l	1006.03			0.18	N IV	1284.22	1284.1	52.98	---
N III	1183.03	1183.3	18.01	0.12	(K) v,p				
(20) w,p	1183.03		18.01	0.24					
	1184.54	1184.8	18.02	0.12	N IV	1296.60	1296.0	52.98	---
	1184.54		18.02	0.60	(K) w,p				
N III	1324.40	1324.7	32.99	---	N IV	1309.56	1309.0	23.32	---
(K) w,p					(K) v,p				
N III	1345.69	1346.2	2.72	---	N IV	1323.98	1324.4	51.85	---
(K) w,p	1346.27		2.71	---	(K) v,p	1325.68	1326.6	51.85	---
	1347.56	---	2.73	---		1326.96		51.85	---
N IV	955.34	953.8	16.13	0.22	N V	1048.20	1048.7	76.28	---
(8) c		955.3			(HA) w,p				
N IV	1078.71	1078.4	52.98	---	N V	1049.65	1048.7	76.29	---
(K) w,p					(HA) w,p				
N IV	1086.08	---	50.11	---	N V	1238.81	1233.3	0.00	0.31
(K) v,p	1086.27	1086.3	50.12	---	(1) c	1242.80	1241.8	0.00	-0.16
	1086.69		50.12	---	O I	1302.17	1302.2	0.00	0.16
N IV	1133.14	1132.9	46.57	---	(2) i,w,l				
(K) w,p	1135.24	---	46.57	---	O III	1138.54	1138.0	26.07	---
	1136.22	1136.4	46.57	---	(K) v,p				
N IV	1168.60		51.85	---	O III	1149.60	1149.0	24.42	---
(K) m,p	1169.06	1168.8	51.85	---	(K) v,p	1150.88	1150.8	24.42	---
	1169.48		51.85	---		1150.77	1153.9	24.42	---
N IV	1188.01	1187.8	48.00	---	O IV	1338.61	1337.6	22.28	---
(K) w,p					(P) c		---		
N IV	1243.73	1244.5	61.71	---		1342.99	1342.2	22.31	---
(K) v,p	1244.92		61.71	---		1343.51	1343.7	22.31	---

Table 2 (cont'd.)

Ion Multiplet	λ(Å) Laboratory	λ(Å) Measured	χ(ev)	gf	Ion Multiplet	λ(Å) Laboratory	λ(Å) Measured	χ(ev)	gf
O VI	1031.91	1025.5	0.00	0.26	Si III	1155.00	---	16.08	---
(1) c	1037.61	1030.3	0.00	0.13	(31) v,p	1155.96	1155.7	16.10	---
		1034.2				1156.78	1156.9	16.10	---
						1158.10	---	16.10	---
Si II	1190.42	1190.9	0.00	0.92		1160.26	1159.4	16.13	---
(5) i,w,p	1193.28	1193.7	0.00	2.00		1161.58	1161.3	16.13	---
Si II	1260.42	1260.6	0.00	3.6	Si III	1172.53	1172.6	16.08	---
(4) i,m					(30) v,p	1174.37	---	16.10	---
						1174.43	---	16.10	---
Si II	1304.37	1304.3	0.00	0.34		1178.00	1178.3	16.13	---
(3) i,w,1									
Si III	993.52	993.6	6.54	0.20	Si III	1206.51	1206.7	0.00	1.68
(6) w,1	994.79	994.8	6.55	0.64	(1) w,1				
	997.39	997.3	6.58	1.00	Si III	1212.01	1212.3	19.02	---
Si III	1083.21	1083.1	15.15	---	(50) w,p				
(23) v,p					Si III	1212.25	1212.3	32.11	---
					(74) w,p				
Si III	1108.37	1108.0	6.54	0.40	Si III	1280.35	1280.1	20.55	---
(5) w,p	1109.94	1110.3	6.55	1.20	(63) w,p				
	1109.97		6.55		Si III	1294.54	1294.2	6.55	---
	1113.17		6.58		(4) w,p	1296.73	1296.0	6.54	---
	1113.20		6.58	2.00		1298.89	---	6.55	1.80
	1113.23		6.58			1298.96	---	6.58	
Si III	1140.54		16.03	---		1301.15	1300.8	6.55	0.40
(32) w,p	1141.58	1142.1	16.10	---		1303.32	---	6.58	0.50
	1142.28		16.10	---	Si III	1212.59	1312.0	10.28	---
	1142.31		16.13	---	(10) w,p				
	1144.96	1144.8	16.13	---	Si IV	1045.50	1045.6	27.06	---
	1145.67		16.13		(21) w,p	1047.27	1048.2	27.08	---
Si III	1145.12		28.55	---					
(41) w,p	1145.15		28.55	---					
	1145.16	1144.8	28.55	---					
	1145.18		28.55	---					
	1145.19		28.55	---					
	1145.22		28.55						

Table 2 (cont'd.)

Ion Multiplet	λ(Å) Laboratory	λ(Å) Measured	χ(ev)	gf	Ion Multiplet	λ(Å) Laboratory	λ(Å) Measured	χ(ev)	gf
Si IV (K) w,p	1051.60	1051.1	---	---	P IV (K) v,p	1161.78	1161.6	29.00	---
Si IV (11) m	1066.63	1066.4	19.88	---	P IV (K) v,p	1197.82	1197.5	31.92	---
Si IV (3) m	1122.49	1122.5	8.84	1.8	P IV (K) v,p	1203.41	1203.0	31.82	---
	1128.32	1127.9	8.90	0.2		1204.30	1204.9	31.81	---
	1128.34		8.90	1.0		1206.51	1206.7	31.80	---
Si IV (16) w,p	1210.65	---	24.05	---	P IV (K) v,l	1264.48	1264.6	29.00	---
	1211.76	1212.2	24.05	---					
Si IV (K) w,p	1280.34	1280.2	---	---	P V (K) v,p	997.64	997.3	25.31	---
	1291.97	1292.3	---	---		1000.36	1000.6	25.31	---
P III (2) v,p	998.00	998.7	0.00	---	P V (H) m	1117.99	---	0.00	1.27
	1003.59	1003.6	0.07	---		1128.01	1127.9	0.00	0.63
P III (K) w,l	1049.82		9.29	---	S II (1) i,v,p	1250.50	1250.8	0.00	0.45
	1050.52	1051.0	9.29	---		1253.79	1254.2	0.00	0.89
	1050.82		9.29	---		1259.53	1259.8	0.00	1.34
P IV (1) w,l	950.67	951.1	0.00	2.75	S III (2) w,l	1012.49	1012.5	0.00	0.30
						1015.51	1014.5	0.04	0.52
P IV (2) w,p	1025.58	---	8.41	---		1015.76		0.04	0.38
	1028.13	---	8.38	---		1021.10	1121.3	0.10	0.38
	1030.54	1030.3	8.47	---		1021.32		0.10	1.12
	1033.14	---	8.41	---	S III (8) w,p	1077.84	1078.4	1.40	---
	1035.54	---	8.47	---					
P IV (K) v,p	1086.94	1086.3	23.47	---	S III (K) v,p	1122.42	---	10.42	---
	1088.61	1089.0	23.47	---		1126.48	1126.7	10.41	---
	1091.44	1091.0	23.47	---		1126.85		10.42	---
P IV (K)	1118.59	1118.9	13.04	---	S III (K) v,p	1155.34	1155.8	10.42	---
						1162.52	---	10.42	---
						1166.13	---	10.41	---

Table 2 (cont'd.)

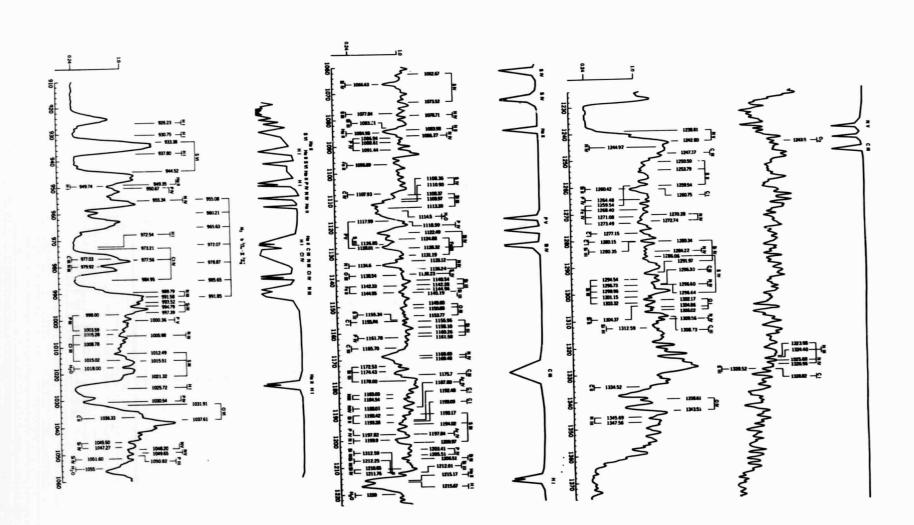| Ion Multiplet	λ(Å) Laboratory	λ(Å) Measured	χ(ev)	gf	Ion Multiplet	λ(Å) Laboratory	λ(Å) Measured	χ(ev)	gf
S III	1189.17	1189.7	0.00	0.42	Ar IV	1187.80	1187.8	4.32	---
(1) w,l	1194.02	1193.8	0.04	0.94	(K) v,p	1190.35	1190.9	4.32	---
	1194.40		0.04	0.32		1197.84	1197.5	4.32	---
	1200.97		0.10	1.77	Fe II	1096.89	1096.3	0.00	---
	1201.71	1200.2	0.10	0.32	(18) i,w,p				
	1202.10		0.10	0.021					
S III	1328.12	1328.8	12.24	---	Fe II	1142.33	1142.2	0.00	---
(K) v,p	1328.52		12.24	---	(10) i,v,p	1143.24	---	0.00	---
						1144.95	1144.8	0.00	---
S IV	1062.67	1063.0	0.00	0.94	Fe III	1122.53	1122.5	0.00	4.50
(1) w,l	1072.99	1073.0	0.12	0.19	(1) w,l	1124.88	1124.8	0.05	2.32
	1073.52		0.12	1.69		1126.72	---	0.09	0.88
S IV	1108.36	1108.0	15.31	---		1128.02	1127.9	0.05	1.17
(K) w,p	1110.90	1110.3	15.31	---		1128.72	---	0.09	1.46
S IV	1138.23	1138.0	15.31	---		1129.19	---	0.12	1.12
(K) v,p						1130.40	---	0.13	0.50
S IV	1286.06	1296.8	16.56	---		1131.19	1131.6	0.12	0.38
(K) v,p	1296.64	1296.0	16.64	---		1131.91		0.09	0.17
S VI	933.38	928.8	0.00	0.5	Fe IV	1254.80	---	20.86	---
(1) c		933.0			(K) w,p	1257.29	---	20.89	---
	944.52	940.8	0.00	1.0		1258.68	---	20.89	---
		945.2				1259.54	1259.8	20.93	---
Cl III	1005.28	1005.0	0.00	0.56		1261.72	---	21.00	---
(1) v,p	1008.78	1009.2	0.00	1.10		1263.47	---	20.93	---
	1015.02	1014.5	0.00	1.66		1265.28	---	21.09	---
Cl IV	973.21	---	0.00	0.55		1268.40	1268.3	21.00	---
(H) w,l	977.56	977.0	0.06	1.24		1271.08	1271.6	21.21	---
	977.90		0.06	0.42		1273.49	1273.0	21.09	---
	984.95	---	0.17	2.32		1280.43	---	21.21	---
	985.75	---	0.17	0.44					

* The eye estimated strength of the feature is strong, s; moderate, m; weak, w; or very weak, v.
∕ The suggested identification is likely, e; or possible, p.
≠ The feature appears as a P Cygni type profile, c; or is probably interstellar in origin, i.

S VI 945 N III 990 Si IV 1067 Si IV 1122 C III 1176 N V 1239 Si II 1304

S VI 933 N₂ EARTH O VI 1032 N II 1084 P V 1128 N I 1135 Lα 1216 Si II 1260 O IV 1339